Tree Physiology 26, 377–388

Hyperhydricity in apple: ultrastuctural and physiological aspects

D. CHAKRABARTY,[1,2] S. Y. PARK,[3] M. B. ALI,[1] K. S. SHIN[1] and K. Y. PAEK[1,4]

[1] *Research Center for the Development of Advanced Horticultural Technology, Chungbuk National University, Cheong Ju, Republic of Korea*

[2] *Present address: Floriculture Section, National Botanical Research institute, Lucknow, India*

[3] *Biotechnology Division, Korea Forest Research Institute, Kwonseon Omockcheon 44-3, Gyunggi Su Won 441-350, Republic of Korea*

[4] *Corresponding author (paekky@chungbuk.ac.kr)*

Received May 16, 2005; accepted June 24, 2005; published online December 15, 2005

Summary We studied the effects of hyperhydricity on subcellular ultrastructure and physiology of leaves during in vitro regeneration of apple plants. Morphological, anatomical and ultrastructural differences between healthy leaf tissues obtained from greenhouse-grown plants and healthy and hyperhydric leaves obtained from shoots raised from nodal shoot explants in a bioreactor were investigated by electron microscopy and confocal laser scanning microscopy. Compared with healthy leaves, hyperhydric leaves showed abnormal, often discontinuous development of the epidermis and cuticle. Stomata were malformed. The leaf lamina appeared thickened and was characterized by poor differentiation between the palisade and spongy mesophyll tissue. Hyperhydric leaves had a significantly lower chloroplast number per cell and chloroplasts showed reduced thylakoid stacking compared with healthy leaves. Hyperhydricity resulted in a general decrease in concentrations of reduced and oxidized pyridine nucleotides, reflecting a reduction in metabolic activity. The activities of antioxidant enzymes, such as superoxide dismutase, catalase, ascorbate peroxidase and glutathione reductase were higher in hyperhydric leaves than in healthy leaves, indicating that hyperhydricity was associated with oxidative stress. Chlorophyll fluorescence measurements provided evidence of oxidative damage to the photosynthetic machinery in hyperhydric leaves: photochemical efficiency of photosystem II, effective quantum efficiency and photochemical quenching were all lower in hyperhydric leaves compared with healthy leaves.

Keywords: antioxidant enzymes, chlorophyll fluorescence, chloroplast, pyridine nucleotides.

Introduction

Micropropagation of woody plants, especially apple (*Malus*) species, is often hampered by the phenomenon of hyperhydricity (vitrification) (Chakrabarty et al. 2003). Hyperhydricity, which is characterized by a glassy or swollen appearance to the tissue, usually results in reduced multiplication rates, poor quality shoots and tissue necrosis (Ziv 1991). The so-called vitrified, vitreous or hyperhydric shoots (HS) appear turgid, watery at their surface and hypolignified. Their organs are translucent, in some cases less green and easily breakable. Anatomical changes observed in hyperhydric leaves include abnormal stomata (Ziv 1991), a reduced number of palisade cell layers, irregular epidermal tissue, large intercellular spaces in the mesophyll cell layer and the presence of a thin cuticle or no cuticle at all (Olmos and Hellín 1998).

Although the occurrence of hyperhydricity remains unpredictable and many factors appear to induce hyperhydricity (Kevers et al. 1984), stress is believed to be the major factor underlying the phenomenon. Stress during in vitro culture could arise as a result of wounding, the properties of the tissue culture medium, infiltration of tissue by the culture medium, which is generally of a high ionic strength and rich in nitrogen and growth regulators, or environmental conditions during in vitro culture in sealed containers (Debergh 1983, Gribble 1999, Thomas et al. 2000). The atmospheric conditions in sealed cultures, which include a high relative humidity, are analogous to those found in association with waterlogged soils and are associated with reduced transpiration and excessive water uptake, which can result in near hypoxic tissue oxygen concentrations and interference with respiration at the level of electron transport.

Photooxidation can occur when plants are exposed to stress and causes damage to the electron transfer system resulting in the formation of reactive oxygen species (ROS; superoxide anion, singlet oxygen, hydrogen peroxide and hydroxyl radical) that attack unsaturated membrane lipids, nucleic acids, enzymes and other cellular structures (Larson 1988, Caasi-Lit et al. 1997). Plants possess antioxidant defense mechanisms against ROS (Larson 1988) that involve various antioxidant compounds (Schöner and Krause 1990) and a battery of antioxidant enzyme systems including catalase (CAT), superoxide dismutase (SOD), peroxidase (POD), glutathione peroxidase (GPX), glutathione *S*-transferase (GST) and the ascorbate-glutathione cycle enzymes (Halliwell 1987, Bowler et al. 1992). It has been suggested that the abnormal morphology of hyperhydric leaves is associated with changes occurring at the cellular level as a result of stress-induced modifications of membrane composition (Franck et al. 1998*b*) or DNA content (Ochatt et al. 2002). However, the relationship between oxidative stress and hyperhydricity has not been established un-

equivocally.

In an attempt to demonstrate the role of oxidative stress in hyperhydricity, we compared chlorophyll fluorescence characteristics and activities of antioxidant enzymes in healthy leaves of greenhouse-grown plants and normal and hyperhydric leaves of in-vitro-grown shoots.

Materials and methods

Plant material

Healthy, fully expanded leaves (third, fourth and fifth from the top) of greenhouse-grown apple plants (*Malus*) 'M9 EMLA' were studied. Nodal cultures of apple 'M9 EMLA' were maintained on MS solid medium (Murashige and Skoog 1962) (3% sucrose + 8 g l^{-1} agar) supplemented with 1 mg l^{-1} 6-benzyladenine (BA), 0.2 mg l^{-1} indole-3-butyric acid (IBA) and 0.8% agar, kept at 25 °C, 70% relative humidity in a 16-h photoperiod at a photosynthetic photon flux (PPF) of 50 µmol m^{-2} s^{-1}. After 4 weeks of culture, nodal segments with one leaf were transferred to the bioreactors.

Bioreactor culture

Nodal segments (25 nodal segments per bioreactor) were transferred to a 5-l balloon type bubble bioreactor (BTBB) containing 1.5 l of MS liquid medium supplemented with 1 mg l^{-1} BA, 0.2 mg l^{-1} IBA and 3% sucrose. The pH of the medium was adjusted to 5.8 before autoclaving. The plant material was supported by a net to avoid complete submersion in the medium. The volume of input air was adjusted to 0.1 vvm (air volume per culture volume per min). The bioreactors and culture vessels were maintained at 25 °C in a 16-h photoperiod at a PPF of 100 µmol m^{-2} s^{-1} (Chakrabarty et al. 2003). Hyperhydric and normal leaves on the in-vitro-grown shoots were sampled after 28 days of culture in the bioreactor.

Leaf relative water content

Leaf relative water content (RWC) was determined on a 1-cm leaf disk as: $(W_{fresh} - W_{dry})/(W_{turgid} - W_{dry})100$, where W_{fresh} is mass of freshly harvested sample, W_{turgid} is turgid mass after saturating the sample with distilled water for 24 h at 4 °C and W_{dry} is the oven-dry (70 °C for 48 h) mass of the sample (Weatherley 1950).

Leaf osmotic potential

Leaf osmotic potential (LOP; MPa) was measured in fully expanded leaves with a WP4 Dewpoint Meter (Decagon Devices, Pullman WA). Leaf discs (1.0 cm), 10 per treatment, were cut from the center of each leaf with a perforator, immediately ground to a powder and the LOP recorded.

Electron microscopy

Leaves were fixed at 4 °C in 2.5% glutaraldehyde and 4% paraformaldehyde in 0.1 M phosphate buffer at pH 7.2; fixed in 1% OsO_4 in the same buffer, dehydrated through an ethanol series and embedded in Spurr's epoxy resin. Ultra-thin sections obtained with a Reichert Ultracut S (Leica, Germany) were stained with uranyl acetate and lead acetate and observed with a Karl Zeiss EM 109 electron microscope (Karl Zeiss, Germany). Semi-thin sections (0.5 mm) were stained with toluidine blue and examined with a Leica light microscope. Chloroplast number was determined from counts in three cells per section on 10 sections.

Confocal laser microscopy

Stomata and adaxial leaf surface of central leaf disks stained with 0.1% acridine orange were examined with a confocal laser system (MRC1024es, Bio-Rad Microscience, Hemel Hempstead, U.K.) comprising a krypton-argon mixed gas laser attached to a Nikon Diaphot-300/200 inverted microscope.

Chlorophyll fluorescence

Chlorophyll fluorescence parameters were measured on the abaxial side of freshly punched leaf disks. Plants were kept in the dark for 30 min before measurement. Fluorescence was measured with a PAM chlorophyll fluorometer (PAM-200, Heinz Walz, Effeltrich, Germany) connected to a leaf clip holder (2030-B, Walz). Minimal fluorescence (F_o) was measured in dark-adapted (30 min) leaves at a PPF of < 0.1 µmol m^{-2} s^{-1} and maximal fluorescence (F_m) was measured after a 1-s saturating pulse (> 3500 µmol m^{-2} s^{-1}) in the same leaves. Maximal variable fluorescence ($F_v = F_m - F_o$) and photochemical efficiency of photosystem II (PSII) (F_v/F_m) of the dark-adapted leaf disks were then calculated. In light-adapted leaves, maximal fluorescence (F_m') was measured after a 1-s saturating pulse (> 3500 µmol m^{-2} s^{-1}) and minimal fluorescence (F_t) was measured when the actinic light was turned off. The fluorescence values measured in light-adapted leaves were used to calculate: variable fluorescence ($F_v' = F_m' - F_t$), non-photochemical quenching ($NPQ = (F_m - F_m')/F_m'$), photochemical quenching ($q_P = (F_m' - F_t)/(F_m' - F_o)$) and effective quantum efficiency ($\Phi_{PSII} = (F_m' - F_t)/F_m'$).

Determination of pyridine nucleotide content

The reduced and oxidized forms of the pyridine nucleotides were extracted from 300 mg fresh mass of leaves with 1 ml of 0.1 M NaOH and 1 ml of 5% (w/v) trichloroacetic acid, respectively, and quantified by the enzymatic cycling method of Matsumura and Miyachi (1980).

Antioxidant enzymatic assays

For determination of antioxidant enzymatic activities, 0.5 g of leaves was homogenized in 1.5 ml of extraction buffer in a pre-chilled mortar and pestle containing liquid nitrogen. The homogenate was filtered through four layers of cheesecloth and centrifuged at 22,000 *g* for 20 min at 4 °C. The supernatant was re-centrifuged and desalted by chromatography through a Sephadex G-25 column equilibrated with the same buffer. The desalted extracts were kept in an ice bath until assayed. Protein concentration of each enzyme extract was determined according to Bradford (1976).

Superoxide dismutase (EC 1.15.1.1) activity was assayed by monitoring the inhibition of the photochemical reduction of nitroblue tetrazolium (NBT) according to the method of Bayer

and Fridovich (1987). Leaves were homogenized in 100 mM potassium phosphate buffer (pH 7.8) containing 0.1 mM ethylenediamine tetraacetic acid (EDTA), 1% (w/v) polyvinyl-pyrrolidone (PVP) and 0.5% (v/v) Triton X-100. One unit of SOD activity was defined as the amount of enzyme required to cause 50% inhibition of the reduction of NBT as monitored at 560 nm. For the determination of ascorbate peroxidase (APX; EC 1.11.1.11), monodehydroascorbate reductase (MDHAR; EC 1.6.5.4) and dehydroascorbate reductase (DHAR; EC 1.8.5.1) activities, leaves were homogenized in 100 mM sodium phosphate buffer (pH 7.0) containing 5 mM ascorbate, 10% glycerol and 1 mM EDTA. The APX activity was determined in 1 ml of a reaction mixture containing 50 mM potassium phosphate (pH 7.0), 0.1 mM ascorbate (extinction coefficient, 2.8 mM^{-1} cm^{-1}) and 0.3 mM H_2O_2. The decrease in absorbance was recorded at 290 nm for 3 min (Chen and Asada 1989). Activity of MDHAR was assayed by following the decrease in absorbance at 340 nm due to NADH oxidation based on an extinction coefficient of 6.22 mM^{-1} cm^{-1} (Hossain et al. 1984). The 1-ml reaction mixture contained 90 mM potassium phosphate buffer (pH 7.0), 0.0125% Triton X-100, 0.2 mM NADH, 2.5 mM L-ascorbic acid and enzyme extract. One unit of ascorbate oxidase is defined by the manufacturer as the amount that causes the oxidation of 1 µmol of ascorbate to monodehydroascorbate per minute.

We assayed DHAR activity by measuring the reduction in dehydroascorbate (DHA) at 265 nm for 4 min (Doulis et al. 1997). The 1-ml reaction mixture contained 90 mM potassium phosphate buffer (pH 7.0), 1 mM EDTA, 5.0 mM glutathione (GSH) and enzyme extract. The reaction was initiated by the addition of 0.2 mM DHA (extinction coefficient, 14 mM^{-1} cm^{-1}). For determination of CAT (EC 1.11.1.6), POD (EC 1.11.1.7), glutathione reductase (GR; EC 1.6.4.2), GPX and GST (EC 2.5.1.18), leaves were homogenized in 100 mM sodium phosphate buffer (pH 7.0) containing 1 mM EDTA. Catalase activity was determined by following the consumption of H_2O_2 (extinction coefficient, 39.4 mM^{-1} cm^{-1}) at 240 nm for 3 min (Aebi 1974). Activity of POD was measured by following the change in absorption at 436 nm due to guaiacol oxidation (extinction coefficient, 6.39 mM^{-1} cm^{-1}) (Pütter 1974). The activity was assayed for 5 min in a reaction solution containing 50 mM potassium phosphate buffer (pH 7.0), 20.1 mM guaiacol, 12.3 mM H_2O_2 and enzyme extract.

The GR activity was assayed by following the reduction of 5,5′-dithio-bis (2-nitrobenzoic acid) at 412 nm (extinction coefficient, 13.6 mM^{-1} cm^{-1}) with the modifications described by Smith et al. (1988). The assay mixture (1 ml) contained 100 mM potassium phosphate buffer (pH 7.5), 1 mM oxidized glutathione, 0.1mM NADPH and 100 µl of enzyme extract. We determined GST activity by measuring the increase in absorbance at 340 nm (extinction coefficient, 9.6 mM^{-1} cm^{-1}), according to Droter et al. (1985). The 1-ml reaction mixture contained 100 mM K-phosphate buffer, pH 6.25, with 0.8 mM 1-chloro-2,4-dinitrobenzene (CDNB) and 10 mM GSH as the substrates.

Activity of GPX was assayed by the oxidation of NADPH at 340 nm (extinction coefficient, 6.22 mM^{-1} cm^{-1}) as described by Pagila and Valentine (1967). The reaction mixture contained 50 mM potassium phosphate buffer, pH 7.0, 1 mM EDTA, 0.24 units GR (EC 1.6.4.2; Sigma-Aldrich, St. Louis), 10 mM GSH, 0.20 mM NADPH and 1 mM sodium azide. After enzyme addition, test tubes were incubated at 37 °C for 10 min and the reaction was then initiated by addition of 1 mM H_2O_2.

Native PAGE and activity stain

Native polyacrylamide gel electrophoresis (PAGE) was performed at 4 °C and 180 V, following Laemmli (1970). For SOD and APX, a 10% polyacrylamide gel was used, whereas a 7% polyacrylamide gel was used to separate CAT. We determined APX activity as described by Mittler and Zilinskas (1993). The gel was equilibrated with 50 mM sodium phosphate buffer (pH 7.0) containing 2 mM ascorbate for 30 min and then incubated in a solution of 50 mM sodium phosphate (pH 7.0), 4 mM ascorbate and 2 mM H_2O_2 for 20 min. The gel was washed in the buffer for 1 min and submerged in a solution of 50 mM sodium phosphate buffer (pH 7.8) containing 28 mM *N,N,N′,N′*-tetramethyl ethylenediamine (TEMED) and 2.45 mM NBT for 10–20 min with gentle agitation in the presence of light. We detected SOD activity as described by Beauchamp and Fridovich (1971). The gel was equilibrated with 50 mM potassium phosphate buffer (pH 7.8) containing 2.8×10^{-5} M riboflavin and 28 mM TEMED for 30 min. The gel was washed in distilled water for 1 min and submerged in equilibration solution containing 2.45 mM NBT for 10–20 min with gentle agitation in the presence of light; the enzymes appeared as colorless bands in a purple background. We determined CAT activity as described by Woodbury et al. (1971). The gel was incubated in 0.01% H_2O_2 for 10–15 min, washed with distilled water twice and then incubated for 15–20 min in 1% $FeCl_3$ and 1% $K_3(Fe(CN_6))$. After staining, the gels were washed with tap water.

ROS measurement

We measured ROS production as the reduction of sodium 3-[1-[phenylamino-carbonyl]-3,4-tetrazolium]-bis (4-methoxy-6-nitro) benzene-sulfonic acid hydrate (XTT) in the presence of O_2^-, with some modifications (Able et al. 1988). Leaves (1 g) were homogenized in 1 ml of 50 mM Tris–HCl buffer (pH 7.5) and centrifuged at 14,000 *g* for 20 min. The reaction mixture contained 50 mM Tris–HCl buffer (pH 7.5), 0.5 mM XTT and 50 µl of protein extract. Reduction of XTT was determined at 470 nm for 4 min. Corrections were made for background absorbance in the presence of 50 units of SOD. The O_2^- production rate was calculated based on an extinction coefficient of 2.16×10^4 M^{-1} cm^{-1}. Production of H_2O_2 was measured spectrophotometrically after reaction with potassium iodide (Alexieva et al. 2001).

Results and discussion

Morphology and anatomy

A large number (28%) of micropropagated apple root stock

'M9 EMLA' shoots cultured in the immersion bioreactor had visible symptoms of hyperhydricity including thick, broad, translucent leaves that were wrinkled or curled, or both, and brittle. The lower dry mass of the hyperhydric leaves compared with healthy leaves from in-vitro-grown shoots indicated that the hyperhydric leaves contained more water than the healthy leaves (93.19 ± 2.24 versus 83.98 ± 2.16%). This was confirmed by the RWC of the tissue, which was significantly higher in hyperhydric leaves (96.03 ± 2.29%) than in healthy leaves of greenhouse-grown plants (69.58 ± 1.23%) and healthy leaves of in-vitro-grown shoots (66.47 ± 1.82%). Excessive water accumulation in plant tissue, the most characteristic symptom of hyperhydricity, can result in depletion of cellular oxygen concentrations. Leaf osmotic potential was more negative in hyperhydric leaves (–1.7 ± 0.05 MPa) than in healthy leaves of greenhouse-grown plants (–0.89 ± 0.04 MPa) and healthy leaves of in-vitro-grown shoots (–1.1 ± 0.1 MPa).

Both healthy and hyperhydric leaves of in-vitro-grown shoots had a thin discontinuous cuticle, with less epicuticular wax compared with healthy leaves of greenhouse-grown plants (Figures 1a–1c). In epidermal cells of healthy and hyperhydric leaves of in-vitro-grown shoots, the plasmalemma is detached from the cell surface at certain points and protrudes into the vacuoles (Figure 1c, arrows). Healthy leaves of greenhouse-grown plants and healthy leaves of in-vitro-grown shoots had a well defined palisade, comprising a single layer of cells and a spongy mesophyll, whereas hyperhydric leaves appeared to have only a spongy mesophyll with large unorganized intercellular spaces (Figures 2a–2c), in agreement with other reports (Vieitez et al. 1985, Jones et al. 1993, Gribble et al. 1996). Healthy leaves of both greenhouse-grown plants and in-vitro-grown shoots had a continous epidermal layer with recessed stomata of normal appearance with kidney-shaped guard cells and a cell wall bordering the protruding, elliptical stomatal pore that was thickened, well defined and ridged (Figures 3a–3c). Hyperhydric leaves had an irregular epidermal layer with abnormal, malformed stomata that were elevated above the leaf surface and wide open (Figures 4a–4c). The guard cells were also abnormal, being elongated rather than round as a result of deformation of the cell plate during division of the primary stomatal mother cells (Figure 3d).

The transmission electron microscope micrographs in Figures 5a and 5b show typical views of normal mesophyll cells and chloroplasts of healthy leaves. There were no major differences between healthy leaves of greenhouse-grown plants and healthy leaves of in-vitro-grown shoots with respect to the cytoplasm, cytoplasmic membranes, number of chloroplasts (12.3 ± 0.57 and 11.6 ± 0.64, respectively), organization or ultrastructure of granal and stromal thylakoids or in other aspects of chloroplast appearance (Figures 5d and 5e). In contrast, hyperhydricity altered the entire ultrastructure of the leaf cells resulting in sparse and disorganized cytoplasm (Figure 5c). The chloroplasts of hyperhydric plants were few in number (3.4 ± 0.14) and contained large starch grains (Figure 5c): sometimes one starch grain occupied the whole plastid (Figure 5f). Most of the chloroplasts had hypertrophied stroma and the intergranal sacs showed evidence of abnormal compression and expansion so that, frequently, the whole

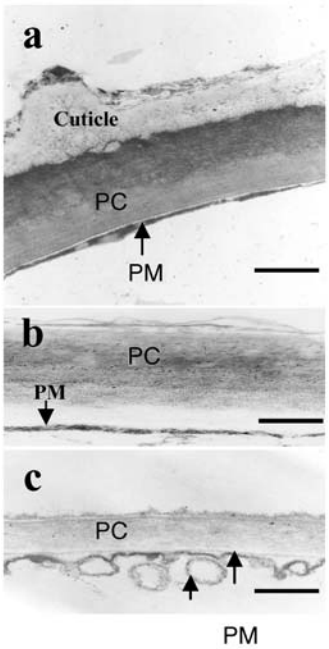

Figure 1. Section of an epidermal cell from (a) a healthy leaf of a greenhouse-grown apple plant; (b) an epidermal cell section from a healthy leaf of an in-vitro-grown shoot; and (c) hyperhydric leaves without epicuticular wax. Abbreviations: PC = primary cell wall; and PM = plasma membrane. Bars = 0.5 µm.

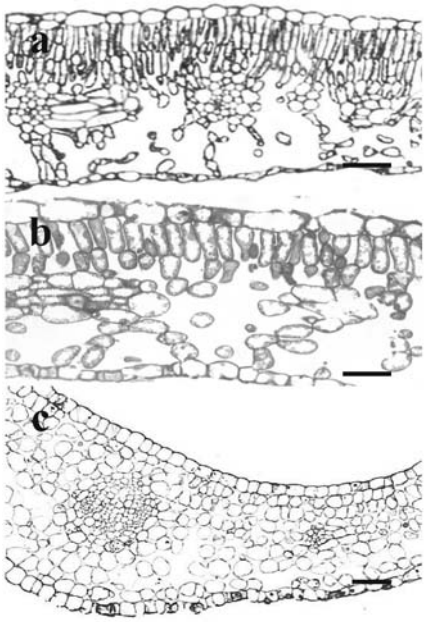

Figure 2. Micrographs of healthy leaves from (a) greenhouse-grown apple plants; (b) in-vitro-grown shoots; and (c) hyperhydric leaves from in-vitro-grown shoots stained with toluidine blue. Bars = 100 µm.

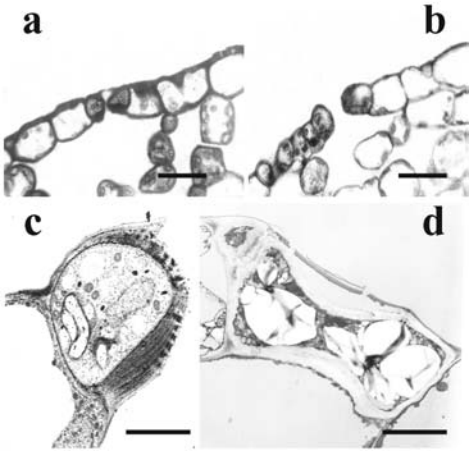

Figure 3. (a) Stomata on a healthy leaf from a greenhouse-grown apple plant (bar = 50 µm) and (b) stomata on a healthy leaf from an in-vitro-grown shoot (bar = 50 µm). (c) Electron micrograph of a guard cell of a healthy leaf from an in-vitro-grown shoot (bar = 1 µm) and (d) electron micrograph of an abnormal guard cell of a hyperhydric leaf (bar = 1 µm).

chloroplast structure was damaged (Figure 5f). In severely hyperhydric leaves, chloroplasts and other subcellular organelles largely disappeared from the cell. Ultrastructurally damaged chloroplasts have previously been observed in hyperhydric leaves of *Prunus avium* L. and carnation and interpreted as a manifestation of autophagy (Franck et al. 1998*a*, Olmos and Hellín 1998). The process of autophagy is a regulated metabolic response that allows cells or tissues to endure a prolonged period of oxidative stress with the best possible chance for survival and growth once favorable conditions are reestablished (Franck et al. 2004). Some evidence of autophagy—which is characterized by autophagic capture of organelles and particles, substantial expansion of the lysosomal compartment and eventual collapse of the nucleus—can be seen in Figure 5c (arrow). Olmos and Hellín (1998) suggested that the altered ultrastructure of hyperhydric leaves is a result of the excessive accumulation of water and the subsequent induction of oxidative stress created under these culture conditions.

Photosynthetic and energetic capacities

A general decrease in reduced and oxidized pyridine nucleotides was observed in hyperhydric leaves compared with healthy leaves (Table 1). Because pyridine nucleotide production is highly dependent on the energetic metabolism of the plant, decreased NADPH production in response to hyperhydricity could reflect low photosynthetic activity, perhaps partly reflecting the reduction in chloroplast number (Figures 5c and 5f), whereas decreased NADH production could be correlated with low respiratory activity. However, because the energy metabolism of in-vitro-cultured plants depends on exogenously added sucrose as a carbon source and sucrose added to the culture medium can inhibit photosynthesis and the Calvin cycle enzymes (Kozai et al. 1991), decreases in the concentrations of NADPH and NADP+ could also reflect the low photosynthetic rates of hyperhydric leaves and healthy leaves of in-vitro-grown shoots compared with healthy leaves of greenhouse-grown plants. Similar observations have been reported in *Prunus avium* by Franck et al. (2001) who suggested hyperhydric leaves had a reduced energy metabolism.

Chlorophylls a and b and carotenoid concentrations were significantly lower in hyperhydric leaves than in healthy leaves (Figure 6A). The decrease in chlorophyll concentration may be associated with the low number of chloroplasts in hyperhydric leaves. Marchner and Possingham (1975) reported that oxidative stress results in a reduction in the number of chloroplasts and our ultrastructural analysis revealed a damaging effect of hyperhydricity on thylakoid membranes (Figure 5f).

We also characterized photosynthetic activity in terms of photochemical efficiency based on chlorophyll fluorescence measurements (Table 2) (Buschmann and Lichtenthaler 1988). Because Φ_{PSII} is the product of the efficiency of the open PSII reaction centers and q_p, the observed decrease in Φ_{PSII} in hyperhydric leaves compared with healthy leaves can be attributed to the decrease in q_p (Figure 6b). This implies that hyperhydricity causes inhibition of electron transport after PSII, because q_p is a proxy for the redox state of Q_A, the primary electron acceptor after PSII. The parallel decreases in Φ_{PSII} and F_v/F_m in response to hyperhydricity (Figure 6b) were likely associated with down-regulation of PSII during steady-state photosynthesis, which suggests additional irreversible damage to the electron transport pathway, perhaps the result of a loss of integrity of the thylakoid membrane as observed in Figure 5f.

Hyperhydricity had no effect on NPQ (Figure 6b), but it significantly decreased F_v/F_m, F_v/F_o, q_P and Φ_{PSII}, indicating that

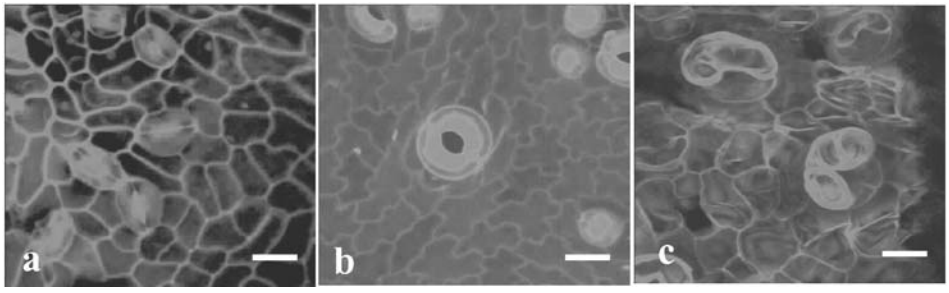

Figure 4. Confocal laser scanning electron micrographs of leaf surfaces: (a) a healthy leaf from a greenhouse-grown plant; (b) a healthy leaf with open stomata from an in-vitro-grown shoot with open stomata; and (c) hyperhydric leaflets with open, abnormal stomata. Bars = 10 µm.

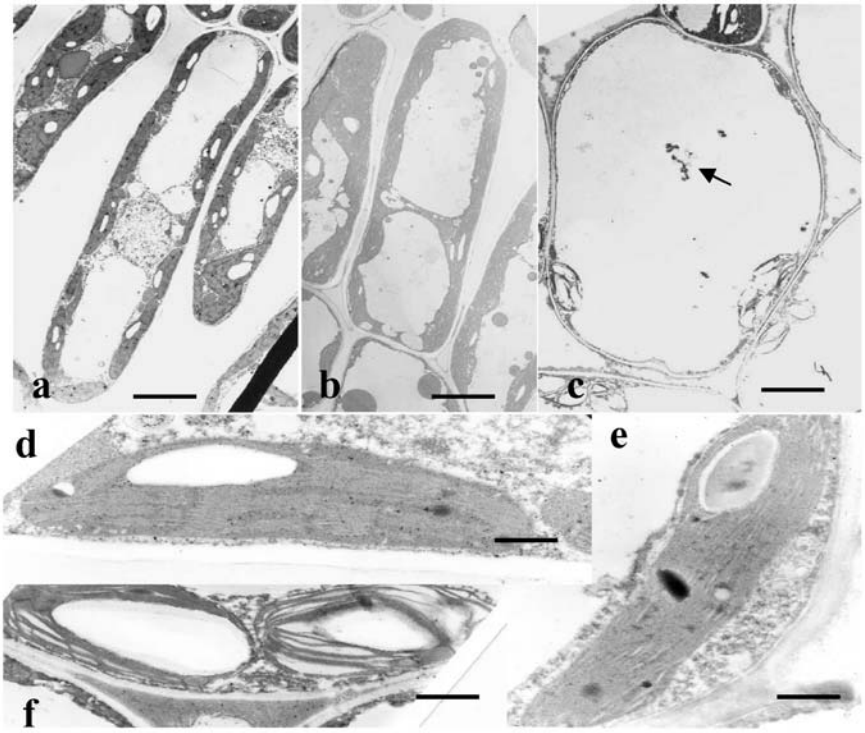

Figure 5. Electron micrograph of a mesophyll cell (bar = 1 μm) from (a) a healthy leaf of a greenhouse-grown apple plant; (b) a healthy leaf of an in-vitro-grown shoot; and (c) a hyperhydric leaf showing details of the autophagic process (Arrow). (d) Section of a mesophyll cell (bar = 0.5 μm) from a healthy leaf of a greenhouse-grown apple plant. Details of chloroplasts (bar = 0.5 μm) in a healthy leaf from an in-vitro-grown shoot (e) and a hyperhydric leaf (f).

a substantial decline of photosynthesis in hyperhydric leaves resulted from a disruption of the photosystem (or at least of PSII) and an accumulation of non-reducing Q_B PSII reaction centers. It has been shown that the key characteristic of these non-reducing Q_B centers is the inhibition of electron transport from Q_A to Q_B (Franck et al. 2002). Increased accumulation of non-reducing Q_B centers in the hyperhydric leaves would inevitably lead to an increase in the fraction of reduced Q_A, thus resulting in a lower q_P, as is observed during photoinhibition. An increased fraction of reduced Q_A suggests that the hyperhydric leaves were subjected to high excess excitation energy, potentially increasing the probability of generating ROS that can damage membrane components of PSII. Thus, the chlorophyll fluorescence measurements indicate that hyperhydricity led to significant oxidative damage to the photosynthetic apparatus. In contrast, Franck et al (2001) reported a slight drop in photochemical process yield in hyperhydric leaves and suggested that a decrease in pigment concentration and not a dysfunction of the photosynthetic apparatus was responsible for the lower photosynthetic capacity observed in hyperhydric *Prunus* shoots.

Table 1. Concentrations of pyridine nucleotides in healthy leaves of greenhouse-grown plants, healthy leaves of in-vitro-grown shoots and hyperhydric leaves of in-vitro-grown shoots of apple rootstock 'M9 ELMA' after 28 days of culture. Within a row, values followed by the same letter do not differ significantly at the 5% level. Abbreviation: DM = dry mass.

	Pyridine nucleotide (nmol g_{DM}^{-1})		
	Greenhouse	Healthy in vitro	Hyperhydric
NAD^+	28.98 a	24.84 a	18.18 b
NADH	5.30 a	5.30 a	1.34 b
$NADP^+$	70.74 a	34.38 b	13.53 c
NADPH	114.53 a	30.48 b	24.37 c
$NADH/NAD^+$	0.18 a	0.21 a	0.07 b
$NADPH/NADP^+$	1.61 a	0.88 b	1.80 a

Antioxidant enzyme activities

To protect the photosynthetic apparatus from oxidative stress, plants dissipate excess light energy. This can be achieved by down-regulation of photochemical efficiency by way of the xanthophyll cycle (Adams and Adams 1996) or by maintenance of electron flux involving alternative pathways such as photorespiration and the Mehler peroxidase reaction (Asada 1999, Ort and Baker 2002). However, both pathways lead to an increased production of ROS and chloroplasts are the main site for generating ROS under both stress and unstressed conditions. We found that hyperhydricity triggered massive ROS production (Figure 7). To cope with ROS, plants possess a complex enzymatic antioxidant system; however, failure of the antioxidant defense system may result in oxidative damage to organelles, such as chloroplasts and cell constituents such as proteins, DNA and membrane lipids (Arakawa et al. 1981, Asada 1999).

Among the ROS, superoxide is converted by SOD into H_2O_2, which is further scavenged by CAT and various peroxidases. The activity of SOD was lower in the healthy leaves of in-vitro-grown shoots than in healthy leaves of greenhouse-grown plants and hyperhydric leaves (Figure 8a). Nondenaturing PAGE coupled with activity localization revealed

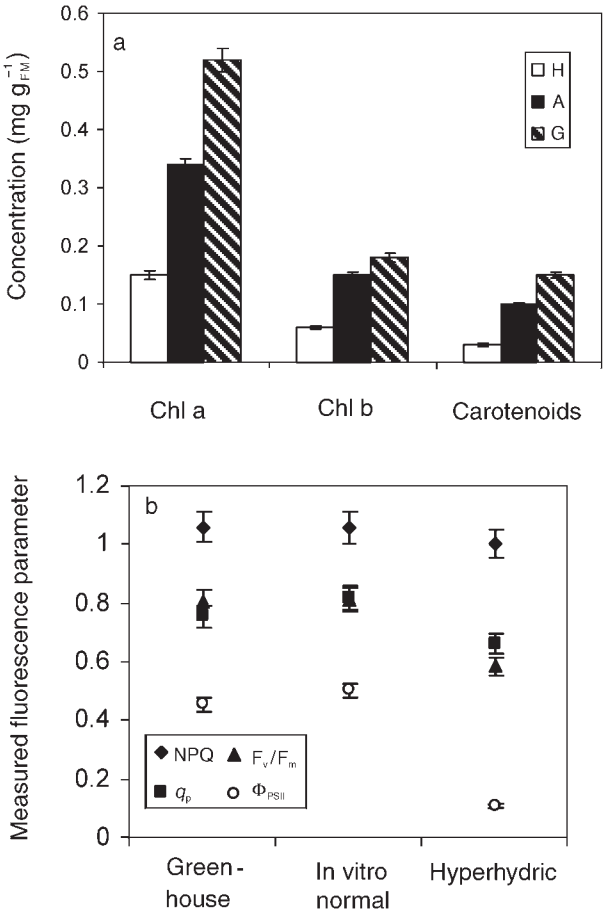

Figure 6. (a) Concentrations of chlorophyll a, chlorophyll b and carotenoids in leaves of apple rootstock 'M9 EMLA' after 28 days of culture. (b) Changes in the photochemical efficiency of photosystem II (PSII) in leaves of apple rootstock 'M9 EMLA' after 28 days of culture. Abbreviations: H = hyperhydric leaf; A = healthy leaf from in-vitro-grown shoot; G = healthy leaf from greenhouse-grown apple plant; NPQ = non-photochemical quenching; q_p = photochemical quenching; F_v/F_m = optimal quantum efficiency; and Φ_{PSII} = effective quantum efficiency.

three SOD isozymes in all leaf types (Figure 8b). Isozymes SOD-2 and SOD-3 were identified as being Mn-SOD and isozyme SOD-1 was a Cu/Zn-SOD. Isozymes SOD-2 and SOD-3 were more prominent in healthy leaves of greenhouse-grown plants than in the other leaf types, whereas SOD-1 was prominent in hyperhydric leaves and to a lesser extent in healthy leaves of in-vitro-grown shoots. It has been suggested that de novo synthesis of antioxidant isozymes with differing kinetic properties could provide an advantage in metabolizing ROS over enhancement of the activities of constitutive antioxidant enzymes (Edwards et al. 1994, Rao et al. 1996). In plants, Mn-SODs are reported to be localized in mitochondria, whereas Cu/Zn-SODs are associated with the cytosol or chloroplast (Baum and Scandalios 1979).

Activity of APX in hyperhydric leaves was high compared with that in healthy leaves (Figure 9a). Examination of APX isozymes revealed five isozymes in hyperhydric leaves (Figure 9B, lane h), of which APX-1, APX-4 and APX-5 appeared to be specific to hyperhydric leaves, being undetectable in healthy leaves of greenhouse-grown plants and in-vitro-grown shoots. Ascorbate peroxidase plays a key role in the ascorbate–glutathione cycle by reducing H_2O_2 to water and producing monodehydroascorbate (MDHA). Because about 90% of the total leaf APX activity is localized in the chloroplast (Gillham and Dodge 1986), this activity likely represents the best estimation of chloroplast-based detoxification of reactive oxygen species through the Mehler-peroxidase pathway.

Activity of CAT was lower in healthy leaves of greenhouse-grown plants and in-vitro-grown shoots than in hyperhydric leaves (Figure 10a). Three well resolved bands of CAT were detected in hyperhydric leaves (Figure 10b), whereas activities of these isozymes were greatly reduced in healthy leaves of greenhouse-grown plants. In hyperhydric leaves, isozymes CAT-1 and CAT-3 were strongly induced, but only faint bands of CAT-1 and CAT-2 activity were detected in healthy leaves of in-vitro-grown shoots (Figure 10b). Catalase eliminates H_2O_2 by converting it to water and oxygen (Winston 1990, Smirnoff 1993). Catalase activity is considered crucial in cellular defence against stress-induced photorespiration

Table 2. Changes in chlorophyll fluorescence parameters in leaf tissues of apple rootstock 'M9 ELMA' after 28 days of culture. Abbreviations: F_o = initial fluorescence in dark-adapted tissues; F_v = variable fluorescence in dark-adapted tissues; F_m = maximum fluorescence in dark-adapted tissues; F_t = initial fluorescence in light-adapted tissues; and F_m' = maximum fluorescence in light-adapted tissues. Within a row, values followed by the same letter do not differ significantly at the 5% level.

	Fluorescence parameter	Greenhouse	Healthy in vitro	Hyperhydric
Dark-adapted tissues	F_o	0.409 b	0.388 b	0.498 a
	F_v	1.717 a	1.694 a	0.7 b
	F_m	2.126 a	2.083 a	1.198 b
	F_v/F_m	0.807 a	0.812 a	0.584 b
	F_m/F_o	5.244 a	5.355 a	2.405 b
	F_v/F_o	4.19 a	4.365 a	1.405 b
Light-adapted tissues	F_t	0.562 a	0.502 a	0.532 b
	F_m'	1.032 a	1.012 a	0.598 b
	$F_m' - F_t$	0.47 b	0.51 b	0.066 a

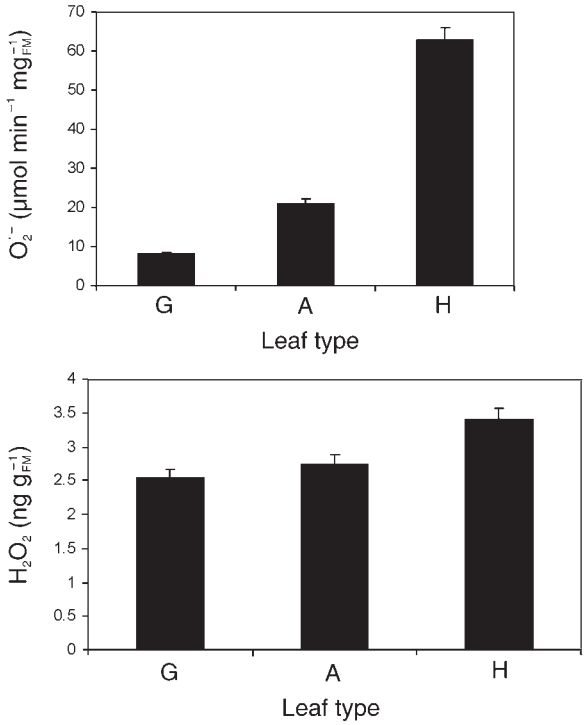

Figure 7. Activity of the reactive oxygen species, O_2^- and H_2O_2, in leaf tissues of apple rootstock 'M9 ELMA' after 28 days of culture. Values are means ± SE (n = 3). Abbreviations: G = healthy leaf from greenhouse-grown apple plant; A = healthy leaf from in-vitro-grown shoot; and H = hyperhydric leaf.

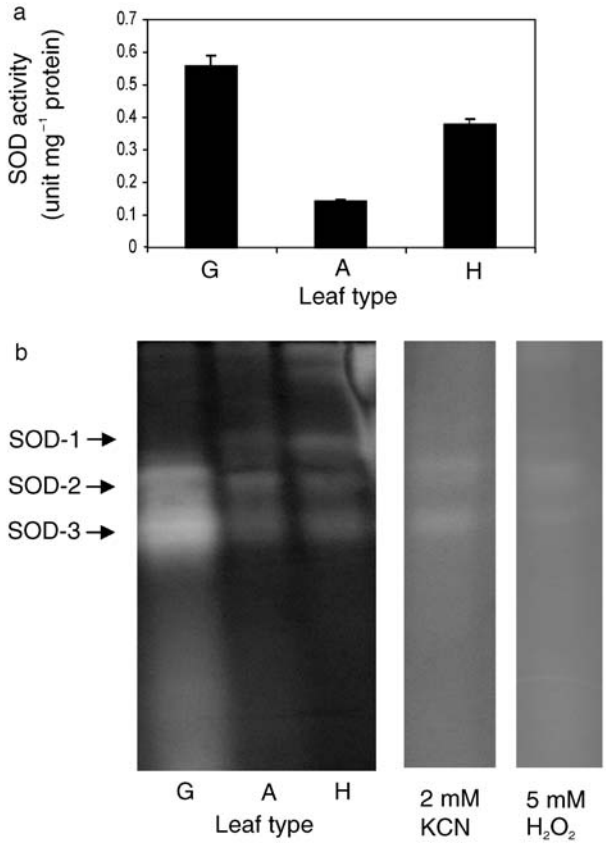

Figure 8. (a) Superoxide dismutase (SOD) activity in leaf tissue of apple rootstock 'M9 ELMA' after 28 days of culture. Values are means ± SE (n = 3). (b) Isoenzyme patterns of SOD activity in leaf tissue of apple rootstock 'M9 ELMA' after 28 days of culture. The different isoforms are numbered from cathode to anode. Equal amounts of protein (150 mg) were loaded in each lane. Abbreviations: G = healthy leaf from greenhouse-grown apple plant; A = healthy leaf from in-vitro-grown shoot; and H = hyperhydric leaf.

in peroxisomes of leaves (Van Breusegem et al. 2001). In transgenic *Nicotiana tabacum* L. with low CAT activity, H_2O_2, arising from photorespiration, is an important mediator of cellular toxicity during environmental stress.

Total POD activity was considerably higher in hyperhydric leaves than in healthy leaves (Figure 11), indicating that POD is likely involved in the antioxidant response against H_2O_2. Similar increases in POD activity in response to hyperhydricity have been observed in other species, including carnations (Olmos et al. 1997).

Hyperhydricity led to significant increases in the activities of GR, GPX and MDHAR (Figure 11). The roles of GR, GPX and glutathione in the H_2O_2-scavenging Halliwell–Asada pathway in plant cells are well documented (Bray et al.

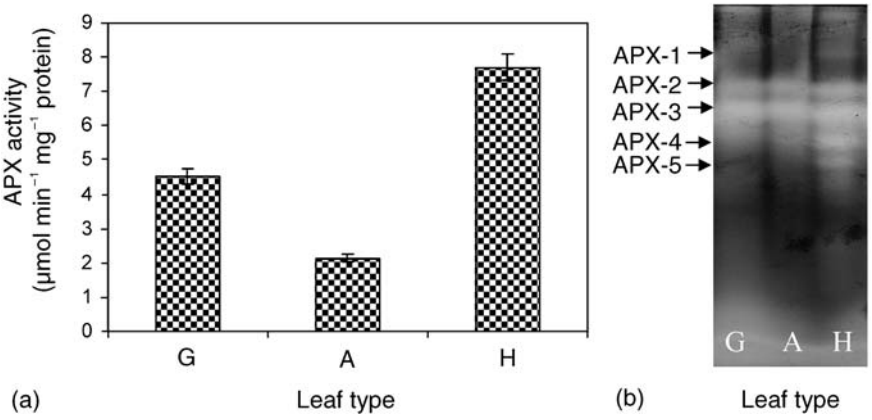

Figure 9. (a) Ascorbate peroxidase (APX) activity in leaf tissue of apple rootstock 'M9 ELMA' after 28 days of culture. Values are means ± SE (n = 3). (b) Isoenzyme patterns of APX activity in leaf tissue of apple rootstock 'M9 ELMA' after 28 days of culture. The different isoforms are numbered from cathode to anode. Equal amounts of protein (150 mg) were loaded in each lane. Abbreviations: G = healthy leaf from greenhouse-grown apple plant; A = healthy leaf from in-vitro-grown shoot; and H = hyperhydric leaf.

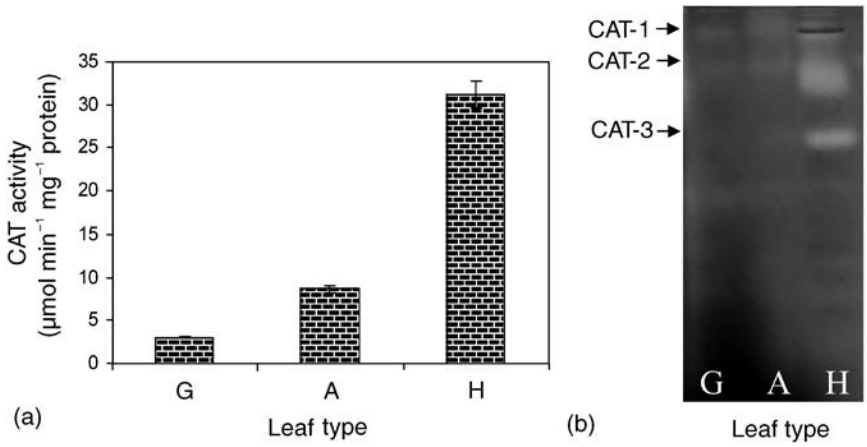

Figure 10. (a) Catalase (CAT) activity in leaf tissue of apple rootstock 'M9 ELMA' after 28 days of culture. Values are means ± SE (n = 3). (b) Isoenzyme patterns of CAT activity in leaf tissue of apple rootstock 'M9 ELMA' after 28 days of culture. The different isoforms are numbered from cathode to anode. Equal amounts of protein (150 mg) were loaded in each lane. Abbreviations: G = healthy leaf from greenhouse-grown apple plant; A = healthy leaf from in-vitro-grown shoot; and H = hyperhydric leaf.

2000): GPX is involved in the removal of hydrogen peroxide and organic peroxides (Flohé and Gunzler 1984) and GR is involved in the recycling of reduced glutathione to maintain a constant intracellular concentration of GSH (Calbert and Mannervik 1985), the main cell antioxidant (Meister 1981, Alscher 1989, Reed 1990). Elevated concentrations of GSH are associated with increased oxidative stress tolerance. Broadbent et al. (1995) found that transgenic plants of tobacco (*Nicotiana tabacum*) overexpressing GR had elevated concentrations of GSH and their leaves had increased tolerance to oxidative stress.

The enzymes MDHAR and DHAR are responsible for ascorbic acid regeneration in plant tissues. The main function of MDHAR is to limit the amount of MDHA undergoing

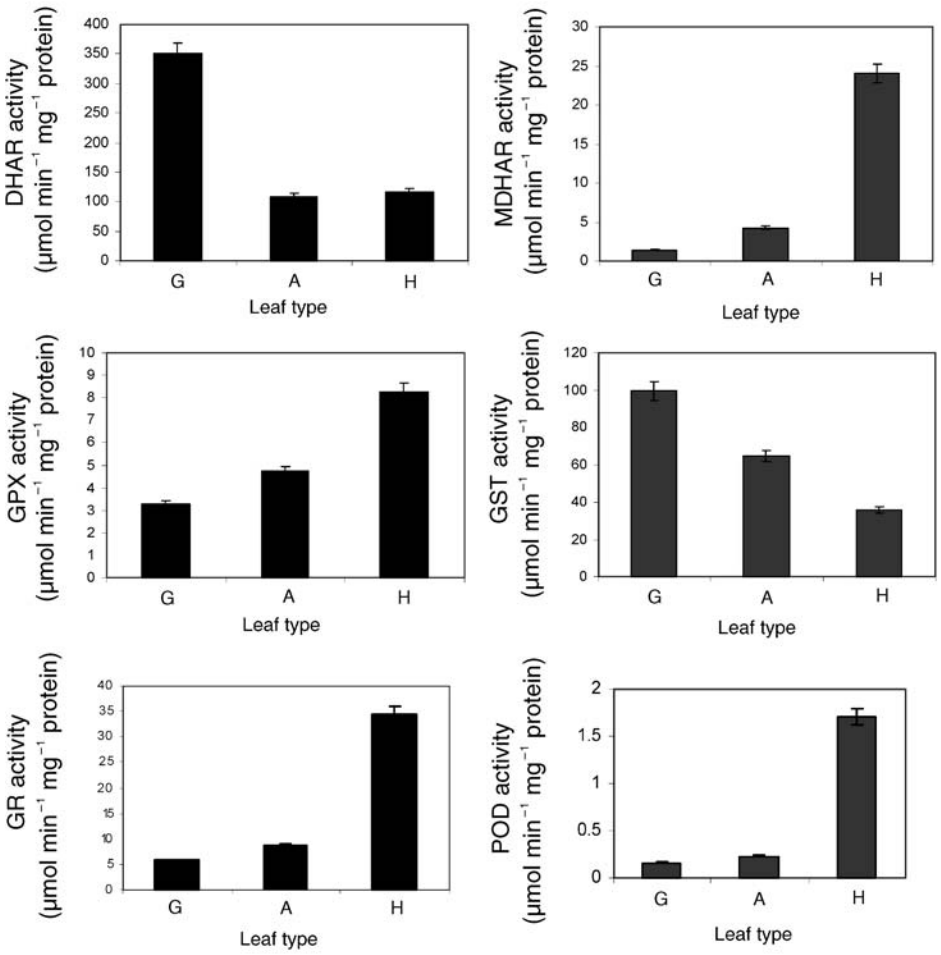

Figure 11. Dehydroascorbate reductase (DHAR), monodehydroascorbate reductase (MDHAR), glutathione peroxidase (GPX), glutathione *S*-transferase (GST), glutathione reductase (GR) and peroxidase (POD) activities in leaf tissue of apple rootstock 'M9 ELMA' after 28 days of culture. Values are means ± SE (n = 3). Abbreviations: G = healthy leaf from greenhouse-grown apple plant; A = healthy leaf from in-vitro-grown shoot; and H = hyperhydric leaf.

non-enzymatic conversion to DHA (Arrigoni 1994, De Gara et al. 2000). We observed a decrease in DHAR activity in hyperhydric leaves and healthy leaves of in-vitro-grown shoots, perhaps reflecting peroxidative enzyme destruction or an inactivation.

The GSTs play an important role in detoxification by catalyzing the conjugation of GSH to toxic substances. Some GST-encoding genes are selectively expressed during abiotic or biotic stress, although several isoenzymes are involved in conjugating natural plant products and can mediate isomerase reactions or function as carrier proteins. In our study, GST activity decreased in response to hyperhydricity (Figure 11), suggesting that it is not involved in detoxification in hyperhydric apple leaves.

Oxidative injury in hyperhydric tissues has been inferred in earlier studies based on higher peroxidase activity, lower lignifications and higher MDA concentration in hyperhydric leaves compared with healthy leaves (Franck et al. 1998*b*, Piqueras et al. 2002, Saher et al. 2004). High relative humidity is considered to be one of the most important environmental factors responsible for hyperhydricity in plants cultured in vitro. The low transpiration and high tissue water content of hyperhydric leaves could result in reduced oxygen uptake leading to hypoxia, disruption of respiratory metabolism and a decline in ATP production. Under hypoxic conditions, some of the metabolic activities that can generate ROS in plants could be disrupted, leading to increased production of ROS and oxidative stress (Asada and Takahashi 1987, Olmos et al. 1997). In contrast, Franck et al. (2004) hypothesize that homeostatic regulation in hyperhydric leaves leads to autophagy or controlled degradation processes that help maintain the integrity and vital functions of the cell for as long as possible under conditions of oxidative stress thereby increasing the chances of survival and growth once favorable conditions are reestablished.

As concluded by Ziv (1991), hyperhydricity involves multiple factors that depend on specific physiological responses to culture conditions as well as the species studied. Hyperhydricity caused substantial ultrastructural damage to apple leaves, especially the chloroplasts. Increased activities of antioxidant enzymes in response to hyperhydricity indicate that this phenomenon caused oxidative injury. The finding that hyperhydric leaves had significantly lower F_v/F_m, F_v/F_o, q_P and Φ_{PSII} than healthy leaves led us to conclude that hyperhydricity caused a substantial decline in photosynthesis in hyperhydric leaves because the antioxidant enzyme system was swamped by a massive accumulation of ROS, the production of which is favored when metabolic pathways are down-regulated. The resulting imbalance between ROS production and antioxidant defenses resulted in oxidative damage of the photosynthetic machinery in the chloroplasts.

Acknowledgments

This work was supported by grants from the Korea Science and Engineering Foundation (KOSEF) to the Research Center for the Development of Advanced Horticultural Technology, Chungbuk National University, Korea. D.C. acknowledges the KOSEF for providing financial assistance under the "Long-term Foreign Scientist Program."

References

Able, A.J., D.I. Guest and M.W. Sutherland. 1988. Use of a new tetrazolium-based assay to study the production of superoxide radicals by tobacco cell cultures challenged with avirulent zoospores of *Phytophthora parasitica* var *nicotianae*. Plant Physiol. 117: 491–499.

Adams, B.D. and W.W. Adams, III. 1996. The role of xanthophyll cycle carotenoids in the protection of photosynthesis. Trends Plant Sci. 1:21–26.

Aebi, H. 1974. Catalases. *In* Methods of Enzymatic Analysis 2. Ed. H.U. Bergmeyer. Academic Press, New York, pp 673–684.

Alexieva, V., I. Sergiev, S. Mapelli and E. Karanov. 2001. The effect of drought and UV on growth and stress markers in pea and wheat. Plant Cell Environ. 24:1337–1344.

Alscher, R.G. 1989. Biosynthesis and antioxidant function of glutathione in plants. Plant Physiol. 77:457–464.

Andersson, B. and S. Styring. 1991. Photosystem II: molecular organization, function and acclimation. Curr. Top. Bioenerg. 16:1–81.

Arakawa, N., K. Tsutsumi, N.G. Sanceda, T. Kurata and C. Inagaki. 1981. A rapid and sensitive method for the determination of ascorbic acid using 4,7-diphenyl-1,10-phenanthroline. Agric. Biol. Chem. 45:1289–1290.

Arrigoni, O. 1994. Ascorbate system in plant development. J. Bioenerg. Biomembr. 26:407–419.

Asada, K. 1999. The water–water cycle in chloroplasts: scavenging of active oxygen and dissipation of excess photons. Annu. Rev. Plant Physiol. Plant Mol. Biol. 50:601–639.

Asada, K. and M. Takahashi. 1987. Production and scavenging of active oxygen in photosynthesis. *In* Photoinhibition. Eds. D.J. Kyle, C.R. Osmond and C.J. Arntzen. Elsevier, Amsterdam, The Netherlands, pp 227–286.

Baum, J.A. and J.G. Scandalios. 1979. Developmental expression and intracellular localization of superoxide dismutases in maize. Differentiation 13:133–140

Beauchamp, C. and I. Fridovich. 1971. Superoxide dismutase: improved assays and an assay applicable to acrylamide gels. Anal. Biochem. 44:276–287.

Bayer, W.F. and I. Fridovich. 1987. Assaying for superoxide dismutase activity: some large consequences of minor changes in condition. Anal. Biochem. 161:559–566.

Bowler, C., M. van Montagu and D. Inze. 1992. Superoxide dismutase and stress tolerance. Annu. Rev. Plant Physiol. Plant Mol. Biol. 43:83–116.

Bradford, M.M. 1976. A rapid and sensitive method for the quantitation of microgram quantities of protein utilizing the principle of protein-dye binding. Anal. Biochem. 72:248–254.

Bray, E.A., J. Bailey-Serres and E. Weretilnyk. 2000. Responses to abiotic stress. *In* Biochemistry and Molecular Biology of Plants. Eds. B.B. Buchanan, W. Gruissem and R.L. Jones. Am. Soc. Plant Biol., Waldorf, pp 1158–1203.

Broadbent, P., G.P. Creissen, B. Kular, A.R. Wellburn and P. Mullineaux. 1995. Oxidative stress responses in transgenic tobacco containing altered levels of glutathione reductase activity. Plant J. 8: 247–255.

Buschmann, C. and H.K. Lichtenthaler. 1988. Reflectance on chlorophyll fluorescence signatures in leaves. *In* Applications of Chlorophyll Fluorescence. Ed. H.K. Lichtenthaler. Kluwer Academic Publishing, Dordrecht, The Netherlands, pp 325–332.

Caasi-Lit, M., M.I. Whitecross, M. Nayudu and G.J. Tanner. 1997. UV-B irradiation induces differential leaf damage ultrastructural changes and accumulation of specific phenolic compounds in rice cultivars. Aust. J. Plant Physiol. 24:261–274.

Calbert, I. and B. Mannervik. 1985. Glutathione reductase. Methods Enzymol. 113:484–490.

Chakrabarty, D., E.J. Hahn, Y.S. Yun and K.Y. Paek. 2003. Micropropagation of apple root stock 'M9 EMLA' using bioreactor. J. Hort. Sci. Biotechnol. 78:605–609.

Chen, G.X. and K. Asada. 1989. Ascorbate peroxidase in tea leaves: occurrence of two isozymes and the differences in their enzymatic and molecular properties. Plant Cell Physiol. 30:987–998.

Debergh, P.C. 1983. Effect of agar brand and concentration on the tissue culture medium. Physiol. Plant. 59:270–276.

De Gara, L., C. Paciolla, M.C. De Tullio, M. Motto and O. Arrigoni. 2000. Ascorbate-dependent hydrogen peroxide detoxification and ascorbate regeneration during germination of a highly productive maize hybrid: evidence of an improved detoxification mechanism against reactive oxygen species. Physiol. Plant. 109:7–13.

Doulis, A.G., N. Debian, A.H. Kingston-Smith and C.H. Foyer. 1997. Differential localization of antioxidants in maize. Plant Physiol. 114:1031–1037.

Droter, A., P. Phelps and R. Fall. 1985. Evidence for glutathione peroxidase activities in cultured plant cells. Plant Sci. 42:35–40.

Edwards, E. A., C. Enard, G.P. Creissen and P.M. Mullineaux. 1994. Synthesis and properties of glutathione reductase in stressed peas. Planta 192:137–143.

Flohé, L. and W.A. Gunzler. 1984. Assays of glutathione peroxidase. Methods Enzymol. 105:141–148.

Franck, F., P. Juneau and R. Popovic. 2002. Resolution of the photosystem I and photosystem II contributions to chlorophyll fluorescence of intact leaves at room temperature. Biochim. Biophys. Acta 45206:1–8.

Franck, T., M. Crèvecoeur, J. Wuest, H. Greppin and T. Gaspar. 1998*a*. Cytological comparison of leaves and stems of *Prunus avium* L. shoots cultured on a solid medium with agar or gelrite. Biotechnol. Histochem. 73:32–43.

Franck, T., C. Kevers, C. Penel, H. Greppin, J.F. Hausman and T. Gaspar. 1998*b*. Reducing properties, and markers of lipid peroxidation in normal and hyperhydrating shoots of *Prunus avium* L. J. Plant Physiol. 153:339–346.

Franck, T., T. Gaspar, C. Kevers, C. Penel, J. Dommes and J.F. Hausman. 2001. Are hyperhydric shoots of *Prunus avium* L. energy deficient? Plant Sci. 160:1145–1151.

Franck, T., C. Kevers, T. Gaspar, J. Dommes, C. Deby, R. Greimers, D. Serteyn and G. Deby-Dupont. 2004. Hyperhydricity of *Prunus avium* shoots cultured on gelrite: a controlled stress response. Plant Physiol. Biochem. 42:519–527.

Gillham, D.J. and A.D. Dodge. 1986. Hydrogen peroxide scavenging systems in pea chloroplasts. Planta 167:246–251.

Gribble, K. 1999. The influence of relative humidity on vitrification, growth and morphology of *Gypsophila paniculata* L. Plant Growth Reg. 27:179–188.

Gribble, A., V. Sarafis, J. Nailon, P. Holford and P. Uwins. 1996. Environmental scanning electron microscopy of the surface of normal and vitrified leaves of *Gypsophila pniculata* cultured in vitro. Plant Cell Rep. 15:771–776.

Halliwell, B. 1987. Oxidative damage, lipid peroxidation and antioxidant protection in chloroplasts. Chem. Phys. Lipids 44:327–340.

Hossain, M.A., Y. Nakano and K. Asada. 1984. Monodehydroascorbate reductase in spinach chloroplasts and its participation in regeneration of ascorbate for scavenging hydrogen peroxide. Plant Cell Physiol. 25:385–395.

Jones, N.B., P.M. Drennan and J. Van Staden. 1993. Leaf anatomy, chloroplast organization and photosynthetic rate of hyperhydric *Eucalyptus saligna* Sm. material. South African J. Bot. 59: 551–555.

Kevers, C., M. Coumans, M.F. Coumans-Gillés and T. Gaspar. 1984. Physiological and biochemical events leading to vitrification of plants cultured in vitro. Physiol. Plant. 61:69–74.

Kozai, T., K. Iwabuchi, K. Watanabe and I. Watanabe. 1991. Photoautotrophic and photomixotrophic growth of strawberry plantlets in vitro and change in nutrients composition in the medium. Plant Cell Tiss. Org. Cult. 25:107–115.

Laemmli, U.K. 1970. Cleavage of structural proteins during the assembly of the head of bacteriophage T4. Nature 227:680–685.

Larson, R.A. 1988. The antioxidants of higher plants. Phytochemistry 27:969–978.

Marschner, H. and J.V. Possingham. 1975. Effects of K and Na on the growth of leaf discs of sugar beet and spinach. Z. Pflanzenphysiol. 75:6–16.

Matsumura, H. and S. Miyachi. 1980. Cycling assay for nicotinamide adenine dinucleotides. Methods Enzymol. 69:465–470.

Meister, A. 1981. Metabolism and functions of glutathione. Trends Biochem. Sci. 231–234.

Mittler, R. and B.A. Zilinskas. 1993. Detection of ascorbate peroxidase activity in native gels by inhibition of the ascorbate dependent reduction of nitroblue tetrazolium. Anal. Biochem. 212: 540–546.

Murashige, T. and F. Skoog. 1962. A revised medium for rapid growth and bioassays with tobacco tissue cultures. Physiol. Plant. 15: 473–497.

Ochatt, S.J., E. Muneaux, C. Machado, L. Jacas and C. Pontécaille. 2002. The hyperhydricity of in vitro regenerants of grass pea (*Lathyrus sativus* L.) is linked with an abnormal DNA content. J. Plant Physiol. 159:1021–1028.

Olmos, E. and E. Hellín. 1998. Ultrastructural differences of hyperhydric and normal leaves from regenerated carnation shoots. Sci. Hort. 75:91–101.

Olmos, E., A. Piqueras, J.R. Martínez-Solano and E. Hellín. 1997. The subcellular localization of peroxidase and the implication of oxidative stress in hyperhydric leaves of regenerated carnation plants. Plant Sci. 130:97–105.

Ort, D.R. and N.R. Baker. 2002. A photoprotective role for O_2 as an alternative electron sink in photosynthesis? Curr. Opin. Plant Biol. 5:193–198.

Pagila, D.E. and W.N. Valentine. 1967. Studies on the quantitative and qualitative characterization of erythrocytes glutathione peroxidase. J. Lab. Clin. Med. 70:158–169.

Piqueras, A., M. Cortina, M.D. Serna and J.L. Casas. 2002. Polyamines and hyperhydricity in micropropagated carnation plants. Plant Sci. 162:671–678.

Pütter, J. 1974. Peroxidases. *In* Methods of Enzymatic Analysis 2. Ed. H.U. Bergmeyer. Academic Press, New York, pp 685–690.

Rao, M.V., G. Paliyath and D.P. Ormrod. 1996. Ultraviolet-B and ozone induced biochemical changes in antioxidant enzymes of *Arabidopsis thaliana.* Plant Physiol. 110:125–136.

Reed, D.J. 1990. Glutathione: toxicological implications. Annu. Rev. Pharm. Toxic. 30:603–631.

Saher, S., A. Piqueras, E. Hellín and E. Olmos. 2004. Hyperhydricity in micropropagated carnation shoots: the role of oxidative stress. Physiol. Plant. 120:152–161.

Schöner, S. and G.H. Krause. 1990. Protective systems against active oxygen species in spinach: response to cold acclimation in excess light. Planta 180:383–389.

Smirnoff, N. 1993. The role of active oxygen in response of plants to water deficit and desiccation. New Phytol. 125:27–58.

Smith, I.K., T.L. Vierheller and C.A. Thorne. 1988. Assay of glutathione reductase in crude tissue homogenates using 5, 5′-dithiobis (2-nitrobenzoic acid). Anal. Biochem. 175:408–413.

Thomas, J., B. Mythili and K.S. Shivashankara. 2000. Explant, medium and vessel aeration affect the incidence of hyperhydricity and recovery of normal plantlets in triploid watermelon. J. Hort. Sci. Biotechnol. 75:19–25.

Van Breusegem, F., E. Vranova, J.F. Dat and D. Inze. 2001. The role of active oxygen species in plant signal transduction. Plant Sci. 161:405–414.

Vieitez, A.M., A. Ballester, M.C. San-José and E. Vieitez. 1985. Anatomical and chemical studies of vitrified shoots of chestnut regenerated in vitro. Physiol. Plant. 65:177–184.

Weatherley, P.E. 1950. Studies in the water relations of the cotton plant. 1. The field measurement of water deficit in leaves. New Phytol. 49:81–97.

Winston, G.W. 1990. Physiochemical basis for free radical formation in cells: production and defenses. *In* Stress Responses in Plants: Adaptation and Acclimation Mechanisms. Eds. R.G. Alscher and J.R. Cumming. Wiley-Liss, New York, pp 57–86.

Woodbury, W., A.K. Spencer and M.A. Stahmann. 1971. An improved procedure using ferricyanide for detecting catalase isozymes. Anal. Biochem. 44:301–305.

Ziv, M. 1991. Vitrification: morphological and physiological disorders of in vitro plants. *In* Micropropagation. Eds. P.C. Debergh and E.S. Zimmerman. Kluwer Academic Publisher, Dordrecht, The Netherlands, pp 45–69.